



Intelligent Secured Two-Way Image Transmission Using Corvus Coron Module over WSN

Bilal Alhayani¹ · Sara Taher Abbas² · Husam Jasim Mohammed³ · Hemant B. Mahajan⁴

Accepted: 13 April 2021 / Published online: 5 May 2021

© The Author(s), under exclusive licence to Springer Science+Business Media, LLC, part of Springer Nature 2021

Abstract

Two-way image communication in a wireless channel needs to be viable with channel properties such as transfer speed, energy-effective, time usage, and security because image capability consumes a huge space in the gadget and is quite effective. Is required in a manner. The figure goes through attacks. In addition, the quiescent issue for additional time of pressure is that the auxiliary interaction of pressure occurs through the dewar receiving extra time. To address these issues, compressed sensing emerges, which packs the image into hours of sensing, is generated in an expedient manner that reduces time usage and saves the use of data transfer capability, however Bomb in transmission. A variety of examinations cleared a way for dealing with security issues in compressive sensing (CS) through giving security as an alternative negotiation. In addition, univariate factors opted for CS as the issue of rearranging image quality is because of the aggregation of clutter. Along these lines related to the above issues, this paper proposed two-way image transmission to the Corvus Coron module, which presents an energy-effective with the CS model, as an inbuilt interaction in the CS transmission through the security framework. Receives what was designated as the pack-protected plot. Impeccable entertainment with the famous arbitrary network conjecture in CS. The result of the test is that the practical module presents energy-efficient and conserved transmission in the form of low error rate with low computational time.

Keywords Chaotic encryption · Manchester coding · MIMO · Wireless channel · Two-way image transmission · Rayleigh fading channel

1 Introduction

Image transmission through a wireless channel needs an image to be viable along the channel attributes, to such an extent that when images along more data are should have been sent over a significant distance, there is a requirement for effective usage of transfer speed [1], lesser force utilization, less time is taken, the negligible measure of room, consequently there emerges a need to pack the data; restricting the repetitive information [2].

✉ Bilal Alhayani
bilalalhayani213@gmail.com

Extended author information available on the last page of the article

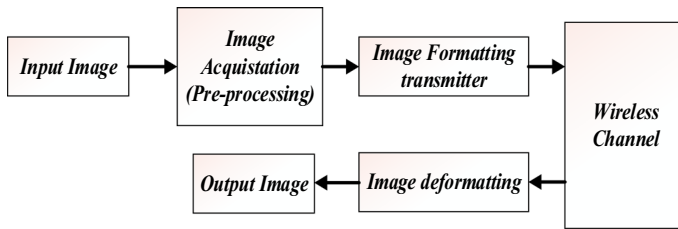


Fig. 1 Example of transmission of image in WSN

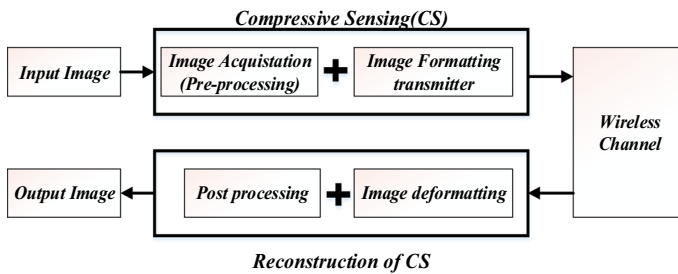


Fig. 2 CS-based image communication in WSN

Degree of compression, distortion rate is some of the factor to be considered, when images are downloaded from the web [3]. Compression leads to the quality of the image being degraded, so to overcome these quality-based issues preprocessing methods like enhancement, segmentation and representation need to be carried out [4]. Once preprocessed, the image gets formatted through various techniques, resulting in digital form. These digital signals consume large space and more time when it moves through a wireless channel [5]. The following figure shows the image transmission process through the channel (Fig. 1).

While image procurement, the accepted signal should be reformatted to acquire the first image sent, however, this sign would likewise incorporate excess data [2]. Thus, a requirement for appropriate pressure strategy which would eliminate this repetitive information is required. [6]. Compressive Sensing (CS) is a sensing methodology that packs the sign gained at the hour of sensing arises and wipes out the repetitive information [7]. Signs can be addressed as inadequate or compressible from different areas [8]. As a result of the meager idea of the signs, the Compressive sensing innovation permits us to test the sign, much underneath the Nyquist rate [9]. Also, the remaking calculations of CS can loyally recreate the first sign back from less compressive estimations [10]. The figure shows the compressive sensing in the channel (Fig. 2).

The primary prerequisite of CS for appropriate recreation is that the estimations should take haphazardly for a legitimate choice of estimation grid. The overall estimation frameworks utilized in CS are the arbitrary networks drawn from Gaussian or Bernoulli dispersion and fractional Fourier lattices [11]. These arbitrary grids are indistinguishable from some other premise, just as submit to the Restricted Isometric Property (RIP) state of wonderful recuperation [12]. If Gaussian dissemination has a place along an orthonormal premise, the lattice will be Gaussian conveyed and consequently, we will want to recuperate the specific arrangement along high likelihood [13]. Albeit, the CS has been assessed alongside irregular estimation networks the issue along arbitrary grids is that we can't store

and repeat them at the collector [14]. This framework should be communicated alongside the sign. So the specialists have redirected their consideration towards the plan of deterministic and organized estimation frameworks that can be utilized as CS estimation grids. Instances of such frameworks are circulant, Toeplitz, organized arbitrary networks, and so forth [15], which has made it conceivable to utilize CS for down-to-earth applications. The benefits of organized arbitrary frameworks are quicker obtaining, lesser capacity necessity, and reproducibility, and decreased transmission overhead, while the downside is its security worry during transmission [16].

CS remaking calculations attempt to discover the scanty assessment of the first input signal, from compressive estimations, in some appropriate premise or outline or dictionary [17]. A great deal of examination has been done on this part of CS, to concoct better-performing calculations. The exploration driving variables around there are the capacity to recuperate from the base number of estimations, commotion power, speed, intricacy, execution ensures, and so forth [8, 18]. Because of the expansion of commotion in the wireless medium, the CS recreation stage crumbles in assessing the arbitrary estimations lattice taken through the CS. Wireless channel experiences blurring and take a multipath engendering to arrive at the collector [19]. These outcomes in debasing the initially communicated signal, subsequently there is a requirement for tweaking the first sign before transmission. Interleaving procedures are crucial for battle the impact of burst mistakes because of blurring, impedance, and multipath engendering in wireless correspondence [20]. Through utilizing linear minimum mean square error (LMMSE) adjustment at the recipient, they broke down the framework through utilizing helical and turbulent interleaving procedures [21]. Because of perceptions utilizing peak signal to noise ratio (PSNR) and root mean square blunder (RMSE) they reasoned that tumultuous interleaving performs better compared to helical interleaving.

16-HQAM (Hierarchical Quadrature Amplitude Modulation) can be utilized for image transmission, which improves the transfer speed effectiveness along the shortfall of dc-part from the sent sign, and Median Filter can be utilized to lessen clamors at channel [22]. HQAM is the high-level form of QAM at a similar information transmission rate along the improved assurance of the particular district in an image from the additional commotion in the channel. The area of interest (ROI) is planned at the main piece and the foundation is planned to the most un-huge piece positions, which improved image quality even at the lower signal-to-clamor proportion. Through the above conversation, plainly in the two-way image transmission, the expansion in the size of a piece pace of images added engendering time, power utilization along bandwidth usage. So for better usage, different pressure methods can be used to lessen the cycle size of an image however the utilization of additional time in pre-preparing brings about the arising of compressive sensing which packs the image through sensing along the idea of dimensional decrease and arbitrary projection. Any data through the channel needs pressure as well as security from the different code assailants like Data Exfiltration, Bad Data Injection, and so forth numerous sorts of exploration cleared a way to address the security issues in CS through giving the security as an optional interaction, proposing that as an inbuilt cycle in CS. Besides, while sending into the channel, the clamor, which added, ought to appropriately gauge on the beneficiary side so the information image could recreate into its unique structure. Hence, for better two-way image transmission, this paper plans a novel module to send the image along less energy utilization and greater security. The blueprint of this paper is summed up as follows. Segment 2 arrangements along related exploration work. Segment 3 talked about the proposed philosophy. Area 4 examined the outcome and execution assessment of this examination and end in segment 5.

2 Related Works

Liao et al. [23] presented another method for distinct information covering up in encrypted pictures using CS and discrete Fourier change. As demonstrated through that technique, CS used to pack and encode secret message parts in order to hide the secret message. The estimate number for CS reproduction monotonically decreases along a decrease in the pressure factor rate. To keep the image exceptionally large, the rate of the suppressor factor must be small. Along these lines, it is not possible to address embedded information and retrieve notable pictures, along a reduction in the estimation number for CS reconstructions.

Ahmad et al. [24] depicted a method considering the captivating properties of the asymmetrical network using the Gram Schmidt figuring. During the time spent square astute self-assertive change, the determined guide was used followed through the dispersal system. The technique makes explicit in encryption and decryption performance using symmetric keys, for example, the encryption and comparative keys (secret keys) used in the uncompressed side. Scrambled images along a secret key may be unbearable along just a comparable secret key. The possibility of spatiotemporal dislocation may extend partners so as to improve the security adequacy of the system. Song et al. [25] introduced two powerful systems for image transmission over dual channels along additional substance burst oscillations shown through the restricted memory polA (transition) channel. Processes, which consider the channel-streamlined scalar quantification (COSQ) of the wave-driven transformation coefficient, misuse channel memory to offer better performance over the various additional astonishing structures expected for the interleaved channel.

Hassen [26] portrayed the square blurring channels along transfer helped distributed spatial variety and uncovered through joint-source – channel coding plans. Lixiang et al. [27] clarified another technique through incorporating QR decay and packed sensing to take care of the reproduction issue of complex networks along the help of the information commotion. The strategy built the estimation lattice along the guide of Gaussian commotion so the scanty information network can be remade through packed sensing. At long last, the work requested without the control input, the strategy for compacted sensing couldn't prevail along regards to reproducing such complex networks in which the conditions of nodes were created through the straight network framework.

The above works recognize significantly testing issues for two-way image transmission. The center thought regarding the Liao et al. [23] and Ahmed et al. [24]. Protecting the image in CS through encryption and decryption, which needs to be communicated. They illustrate the way images are ensured through symmetric key planning and transformation interactions, although neglecting their functions to focus the remaking of unique information along less quantitative.

In like manner, issues in the channels are distinguished and to some degree amended through crafted through Song et al. [25], Hassan [26], and Lixiang et al. [27]. From the nitty-gritty examination, it comes to realize that there is as yet ailing in the papers for giving security as an inbuilt cycle in CS and the legitimate assessment of clamor in the irregular quantifiable of the reproduction stage [28–30].

3 Proposed Methodology

3.1 System Design

The two-way image communication framework emerges the issue of burning-through more energy because of the huge transfer speed use through a colossal number of pieces and goes through different interaction like securing, pressure, the change needs extra computational time along these lines, way decreases the speed of the handling time. Subsequently, to defeat as a joined hotspot for procurement, pressure, and change, the idea of compressive sensing is used through their tendency of dimensional decrease and irregular projection, which detected itself and lessens the transfer speed use. Concerning CS, the underlying choice of irregular factors for image obtaining is a significant factor because the ill-advised determination of arbitrary factors in CS makes confound to recover the image because of the expansion of comotion and inferable from the idea of the dimensional decrease and arbitrary projection, the method doesn't hold the security boundaries though if the security gave after the pressure interaction, it takes additional time. Thus, to extricate the above all around said issues cleverly, the exploration has curiously proposed a Corvus Corone two-way image transmission module. This module performs less data transmission use through quantization along choosing the irregular variable in the spatial space as a regularized structure utilizing least squares models and uncovers a considerable sum about the conduct of the assessors in de-quantization. Figure 3 shows the proposed two-way helpful image transmission model. In addition, the dispersion and dispersion of a Tughlaq property in a booby ringer is used as a planning condition in quantization, claiming to see only those familiar along the language of the pixies so that the image bits. Image attackers later provide high security to image bits. To send these pieces along bending without a signal, at that point, the idea of modulation for broadcasting in the

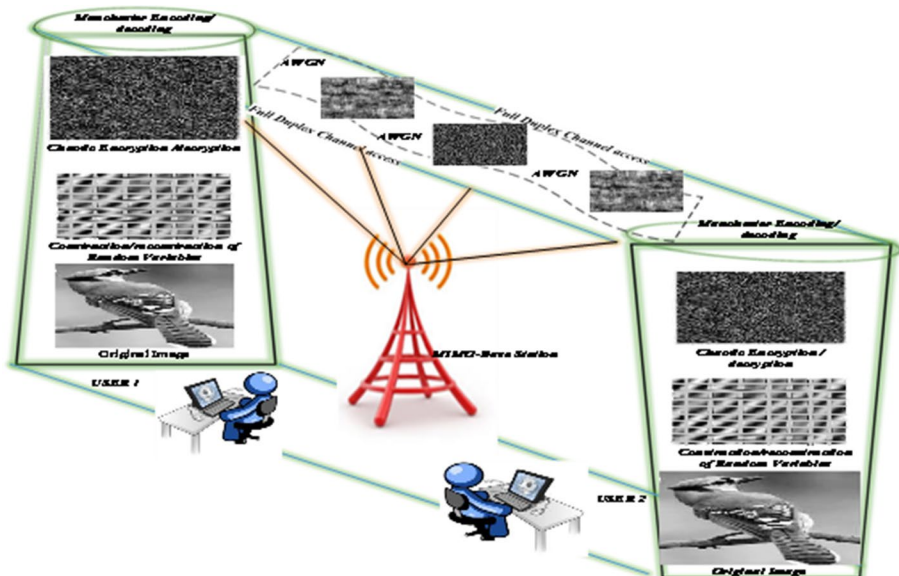


Fig. 3 Architecture of Corvus Corone based two-way image transmission

MIMO channel needs to be met, which is allowed to arrive in the full-duplex channel that communicates in two ways.

The additive white Gaussian noise (AWGN) is added when communicating through the channel, so it can be properly squeezed into the remaking stage to retrieve the first encoded bits. Appropriately, in this proposed module, the use of mid-rate bit coding of modulation can reproduce the first fragments along their clock property through realizing the state of the first pieces and the paired clutter state. As a result, clever modules will reduce the need for new separation strategies, which burn along extra time, here. Through normal construction, the Corvus Coron module delivers superior energy effectiveness and achieves two-way image transmission through its cycle of volume along safety and transmission. The general plan of the proposed two-way image transmission is depicted below. In Fig. 3, client 1 and client 2 associates along two-way correspondence through the proposed Corvus Coron Module transmission framework. On the transmitter side, the client sends the image through developing the arbitrary variable as a packed structure from the first image, and afterward utilizing the turbulent property of the dabbling ringer the factors in the image get scrambled. The numerical clarification for the proposed module is given beneath in the accompanying area.

3.2 Image at Transmitter

Let us consider the image I_m which has to be transmitted through the users is given through the Eq. (1) as,

$$I_m = \begin{bmatrix} P_{1,1} & P_{1,2} & P_{1,j} \\ P_{2,1} & P_{2,2} & P_{2,j} \\ \vdots & & \\ P_{i,1} & P_{i,2} & P_{i,j} \end{bmatrix} \quad (1)$$

Here $i, j = 1, 2, 3, \dots, n$. If the image is transmitted from user 1 to user 2, due to the high number of bits in I_m , the bandwidth usage in the channel increases thus increasing the energy requirement and affecting the entire transmission system. So to get energy efficient and low bandwidth usage, the required image I_m needs to be compressed. Now, the proposed module introduced a security matrix in CS as an inbuilt process that was designated as a compressed security matrix. To generate a compressed safety matrix,, C ', Image I_m In Eq. 5, the random measurement matrix is multiplied together along the input image and the security matrix which can be described mathematically and are given below.

$$C = a\bar{\omega}I_m \quad (2)$$

where $\varpi \in I_m^{i \times j}$ or $P_{ij}^{i \times j}$ is the random measurement matrix, $c \in I_m^{i \times j}$ or $P_{ij}^{i \times j}$ is the compressed security measurement vector of length i and $a \in I_m^{i \times j}$ is the security matrix of area $i \times j$. Here, the number of measurements taken are much lesser than the length of input image, i.e., $i < j$. The size of measurement matrix and the number of measurements is proportional to the sparsity of input signal. The procedures for constructing the compressed secured matrix using the proposed module are given below:

3.2.1 Step 1: Sensing Input Image for Transmission

The input image I_m is sensed for the transmission which can represented through the pixel value P_{ij} . The property of the pixel P_{ij} is given through

$$P_{ij} = \begin{bmatrix} a_1 & a_2 & a_m \\ b_1 & b_2 & b_m \\ \vdots & & \\ z_1, & z_2, & z_m \end{bmatrix} \quad (3)$$

Here a, b, ..., z represents the features of the image I_m .

3.2.2 Step 2: Construction of Random Measurement

In the construction phase of the proposed module, it is important to select random measurements because improper selection of random measurements leads to incomplete retrieval of the image. Random measurements are therefore constructed to improve the prediction accuracy and the interpretation of the regression model through altering the fitting process of the model. Let us consider the features from the image pixel $P_i = [a_i, b_i, c_i, \dots, z_i]$ and construct the random measurable for ϖ_i is given through:

$$\varpi_i = \frac{1}{N} \sum_{i=1}^N f(P_i, P_{ij}, \tau, v) \quad (4)$$

where $P_i = (P_i)^T$ are predictive features variable, x_i are responses and retrieved parameters for prediction accuracy and interpretation. In Eq. 4, the module selects a subset of covalents to achieve both of these goals, the sum of the absolute values of the regression coefficients being a smaller amount than a fixed value, which drives some coefficients to be set to zero. Is, effectively choosing a simple model where the coefficient is not included. Through selecting these coefficients along predictive accuracy and interpreting the parameters, random variables can be easily identified and reconstructed in the final step. To protect these variables from various cipher attacks, the need for encryption arises, which can be explained in the following procedure.

3.2.3 Step 3: Construction of Security Matrix

The security matrix along a 2-D discrete-time dynamic system obtained from Eq. 5 is subject to the current chaotic values A_l , followed through the next chaotic values binding its control parameters p, q, r, s, which helps to confuse.. and the attackers are given through equations

$$a_{i+1} = a_i^2 - b_i^2 + pa_i + qb_i \quad (5)$$

$$b_{i+1} = 2a_i b_i + ra_i + sb_i \quad (6)$$

The initial values are assumed to be a_0, b_0 and parameters $p=0.9, q=-0.6013, r=2.0, s=0.50$. Through their confusion and diffusion property along the features, the pixel values in the image are encrypted and are protected from attackers of each and every kind in the image pixel. The chaotic values of Eq. (5) and (6) make the pixels in tinkering bells in encrypted form and provide confusing information about the data, adding more complexity to attackers. The following mathematical evaluation was then performed to produce the compressed safe form of an image.

3.2.4 Step 4: Creation of Compressed Secured Image

In accordance along the above design the input scenario from the image in Eq. 1, the matrix formed through the random medial in Eq. 5 and the chaotic values obtained in Eqs. 5 and 6 are multiplied and the compressed safe matrix output given through Eq. 7 creates the output:

$$c_i = \begin{bmatrix} a_i \\ b_i \end{bmatrix} \left[\frac{1}{N} \sum_{i=1}^N f(P_{ij}, x_i, \tau, v) \right] \begin{bmatrix} p_{11} \\ p_{12} \\ p_{1j} \end{bmatrix} \quad (7)$$

Through the above Eq. 7, the obtained matrix is in the compressed form of:

$$c_i = \begin{bmatrix} c_{11} \\ c_{12} \\ c_{1j} \end{bmatrix}. \quad (8)$$

Accordingly as expressed over, the image is compacted as a solitary framework, subsequently the quantity of pieces gets decreased, which in-turns produce energy-proficient transmission along less use of data transfer capacity. Additionally through the change of the pixel esteems into turbulent qualities, every one of the pixels get scrambled, subsequently it shields the image information from the aggressors. The pseudo-code for the development for packed security is given in Fig. 4. Figure 4 clarifies that in the primary stage the image that must be communicated is chosen through addressing every one of the qualities as a pixel portrayal. At that point the arbitrary estimation chose as a unit line or section grid gets used. At long last, for security, tumultuous qualities are produced, and through the multiplicative factor, the last packed got grid is shaped. Presently the compacted got yield must be communicated into the MIMO channel along the goal that client 2 can get the image of client 1.

3.2.5 Image Transmission Using MIMO

To improve framework limits and dependencies, the module uses the MIMO method. Along the advancement of radio wire, MIMO and interruption alternation methods, it is possible to understand synchronous transmission on a similar band simultaneously. In addition, the clandestine terminal issue, the interruption issue brought about through the MAC scheme, and the huge postpone issue in multi-jump wireless networks can be fixed in MIMO. The boundaries considered for the direct transmission appearing in Table 1. The process of image transmission via MIMO explained in Fig. 5.

Modulation encoding exercises the inverse in the middle of each bit interval for both synchronization and bit representation. Using a dual-purpose single transition, modulation encoding achieves the same level of synchronization as RZ along only two dimensions. According to existing coding methods, the modulation code overcomes an algorithm for data encoding. This algorithm performs as follows: The data representation is the line transition. A logic 0 is denoted through a transition from high to LOW, and an argument is vice versa. The representation of the modulation encoder is given through

$$K(t) = c_i \oplus CL \quad (9)$$

Through obtaining the number of bits the BPSK modulation done for the full duplex MIMO channel which is given through

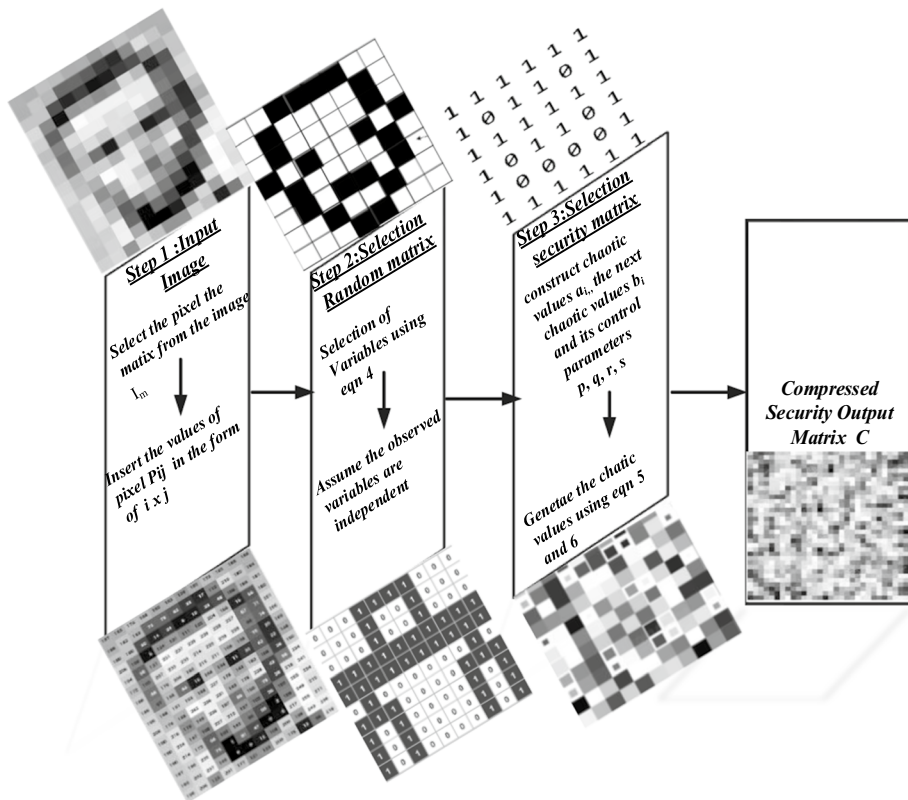


Fig. 4 Functionality of compressed security matrix

Table 1 Parameters for MIMO image transmission

Terms	Method considered
Transmission/receiving scheme	MIMO
Channel access	Full duplexing
Modulation scheme	BPSK
Coding scheme	Modulation coding
Fading channel	Rayleigh fading channel
Noise considered	Additive white Gaussian noise (AWGN)

$$\varphi(t) = K(t) \sqrt{\frac{2}{b_s}} \cos(2\pi q_c t) \quad (10)$$

where $2\pi q_c t$ frequency term, b_s is the number of bits per seconds.

For image communication, the framework comprises two nodes, and every node has two reception apparatuses that can send and get information. Regarding a node, the MIMO sending the signal-modulating module converts the advanced signal into two branches. This framework allows the node to communicate and receive all parcels and

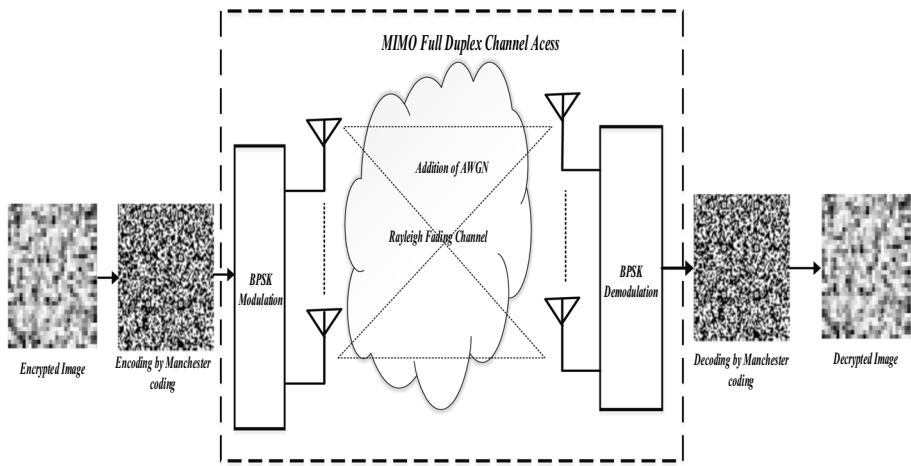


Fig. 5 Illustration of image transmission via MIMO

can improve the unbreakable quality and information rate of the framework through additional coding and space diversity processes. In view of adjusting the signal, they are routed through the Rayleigh blurring channel, and AWGN noise is added. Through using the MIMO channel along full-duplex access, the framework's dependency and information speed are improved. BPSK modulation is completed for coding modulation. The diagram diagram for the broadcast channel is given below:

To recuperate the first image, the remaking eliminate is conveyed that can be clarified in the accompanying segment.

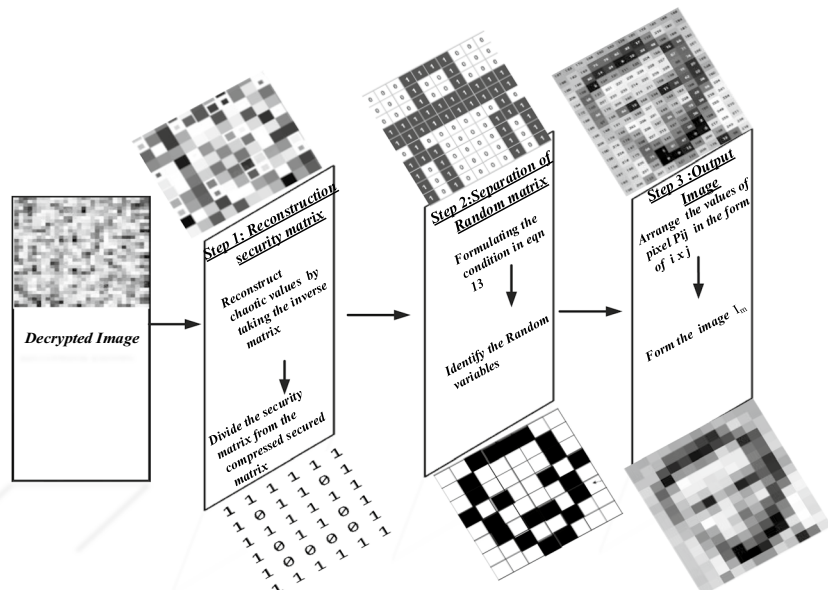


Fig. 6 Original image reconstruction

3.2.6 Image Reconstruction Phase

After transmitting the adjusted image signal to the MIMO channel along full-duplex access, the signal is expanded from the channel to the AWGN's Rale Fading channel

$$\phi(t) = \varphi(t) + e \quad (11)$$

where e is the AWGN, The noise that added could estimate properly, so that it is easy to regain the original modulated signal. The estimation noise in the channel given through

$$e = \frac{1}{2} \pi q_c t \left(\sqrt{\frac{U}{V}} \right), \quad (12)$$

Here $\frac{U}{V}$ is the signal to noise ratio. The retrieval of the modulated signal along the estimation of the noise in Eq. (5) given through

$$\hat{\varphi}(t) = \phi(t) - \frac{1}{2} \pi q_c t \left(\sqrt{\frac{U}{V}} \right) \quad (13)$$

The signal get demodulated through the BPSK that is given through

$$\hat{K}(t) = \frac{\hat{\varphi}(t)}{\sqrt{\frac{2}{b_s}} \cos(2\pi q_c t)} \quad (14)$$

After the signals are collapsed in the remaking phase, the signal that is encoded along the modulation coding is decoded through the modulation's clock recoupment property.

$$\hat{c}_i = CL \oplus \hat{K}(t) \quad (15)$$

Presently the first adjusted sign gets decoded. At that point to recover the first image the accompanying precise strategies were used through isolating every lattice to acquire the first image. The choice of safety grid can unscramble through the converse capacity of the tumultuous benefits of the fiddling chime. Through knowing the underlying tumultuous qualities, the decoding of the lattice is finished through the qualities which have been set done at first is given through

$$\hat{\alpha} = \begin{bmatrix} a_i \\ b_i \end{bmatrix}^{-1} \quad (16)$$

Then the random matrix, which was obtained through the condition of the regression principle can be predicted through

$$\hat{\varpi} = Min = \frac{1}{N} \sum_{i=1}^N f(P_{ij}, C_{ij}, \tau, v) \quad \text{Subjected to} \quad \|v\| < t \quad (17)$$

Hence through foreseeing the arbitrary grid through the relapse rule, unscrambling the tumultuous qualities and the legitimate assessment of commotion, the first image got in the recreation stage is given through relating the condition 11, 12, and 13 is



Fig. 7 Graphical user interface model



Fig. 8 Input images

$$I_m = \frac{\hat{c}_i}{\hat{\omega} \hat{\alpha}} \quad (18)$$

where I_m is the original image reconstructed through the proposed Corvus Corone Module. The pseudo code for the reconstruction phase of the proposed module is showing in Fig. 6.

Figure 6 clarifies that to unscramble the image, the reproduction of the compacted got lattice is completed, at which the reverse estimation for the tumultuous benefits of the fiddling ringer is determined at first, and afterward utilizing the expectation of the relapse guideline the irregular framework are remade precisely. This guideline assists along getting the first image as a yield. The general calculation for the proposed Corvus Corone Model is given underneath in Algorithm 1.

Algorithm 1: Secure image transmission

Input: Image: I_m

Output: Image: I_n

Stages: Construction, Transmission, Reconstruction

Stages 1 : Construction of compressed security matrix

$C = \alpha \bar{\omega} I_m$, through details

Let $I_m = \{P_1, \dots, P_n\}$ I_1, \dots, I_n Image pixels

If, Random matrix $\bar{\omega} \in I_m^{i \times j}$ or $P_{ij}^{i \times j}$,

For $\bar{\omega}_i = \frac{1}{N} \sum_{i=1}^N f(P_i, P_{ij}, \tau, v)$

Then, if Security Function $\alpha \in I_m^{i \times j}$

For $a_{i+1} = a_i^2 - b_i^2 + pa_i + qb_i$ & $b_{i+1} = 2a_i b_i + ra_i + sb_i$.

Construct the compressed secured matrix:

$$c_i = \begin{bmatrix} a_i \\ b_i \end{bmatrix} \left[\frac{1}{N} \sum_{i=1}^N f(P_{ij}, x_i, \tau, v) \right] \begin{bmatrix} p_{11} \\ p_{12} \\ \vdots \\ p_{1j} \end{bmatrix}$$

End

End

Stages 2 : Transmission through MIMO channel code

$K(t) = c_i \oplus CL$,

Modulate, $\emptyset(t) = K(t) \sqrt{\frac{2}{bs}} \cos(2\pi q_c t)$

Stages 3 : Reconstruction of original image

For,

$\theta(t) = \emptyset(t) + e$

$$\hat{K}(t) = \frac{\hat{\theta}(t)}{\sqrt{\frac{2}{bs}} \cos(2\pi q_c t)}$$

$$\hat{c}_i = CL \oplus \hat{K}(t)$$

End,

Reconstruct the matrix,

decrypt through the inverse function of the chaotic values of tinkering bell

$$\text{If, } \hat{a} = \begin{bmatrix} a_i \\ b_i \end{bmatrix}^{-1}$$

Get decode the random matrix, which was obtained

$$\bar{\omega} = \min_{t, v} = \frac{1}{N} \sum_{i=1}^N f(P_{ij}, C_{ij}, \tau, v) \quad \text{Where } \|v\| < t$$

The output original image obtained in the reconstruction

$$I_n = \frac{\bar{C}_i}{\bar{\omega} \bar{a}}$$

End

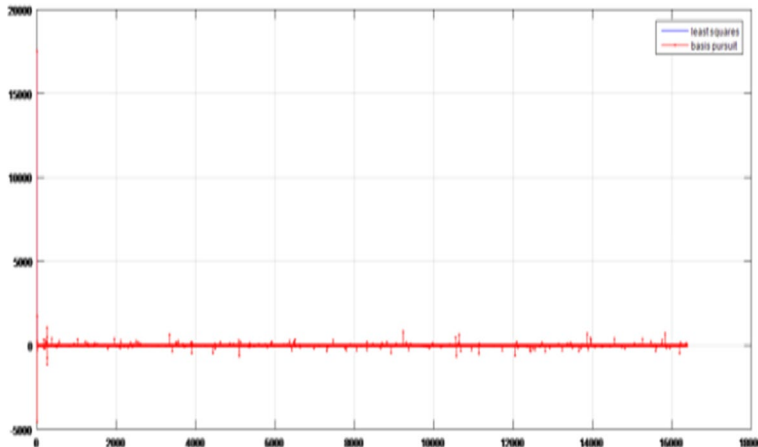


Fig. 9 Selection of random variables for input image (Camera-man)

Through the general plan of the proposed, the huge quantities of image bits get compacted through the packed gotten grid, that helps in less data transfer capacity usage in the meantime creating the Energy-producing transmission, and the assets found in the framework make it complicated for the aggressor to hack the image. The intelligent determination of irregular factors through the prediction and integrality property of the forecast standard reproduces the image precisely in the reproduction phase. The transmission of signals in the MIMO channel through full-duplex channel access and

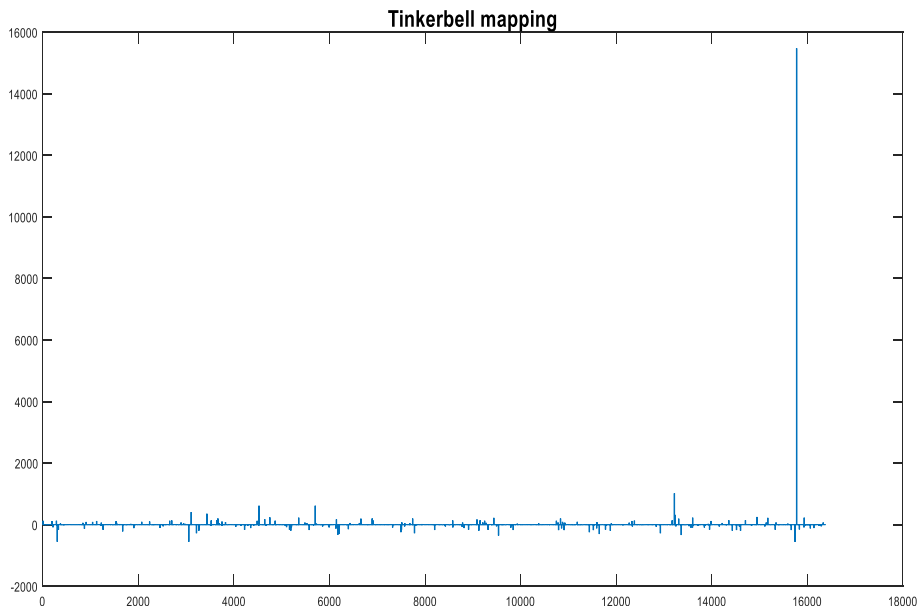
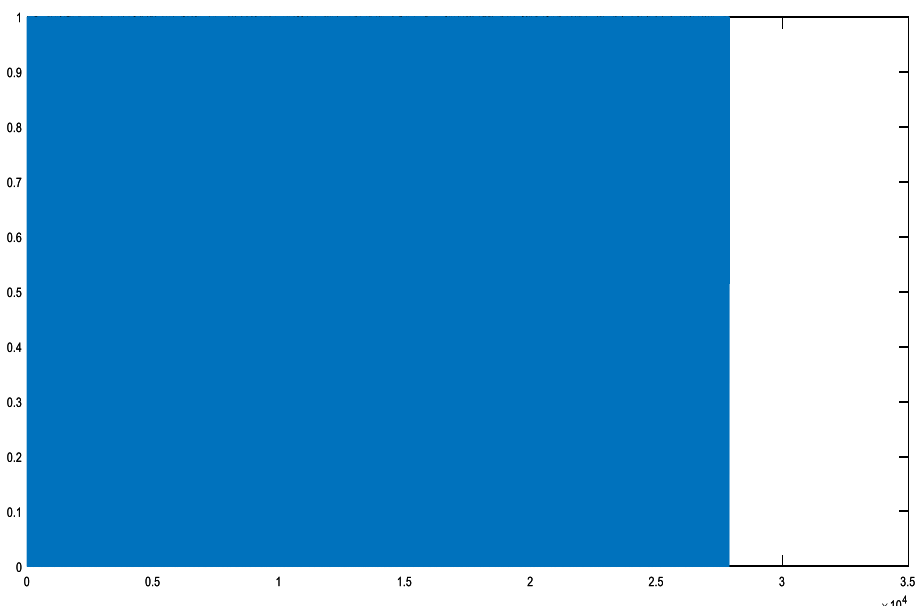


Fig. 10 Construction of security matrix of input image (camera man)

Table 2 Processing parameter

Parameter	Description
Channel type	Downlink/uplink
Number of transmitting station	2
Number of receiving station	2
Number of users	2
Number of bits transmitted	1024 bits/packets
Bit rate	1 kb/s
Modulation scheme	BPSK (Manchester coding)
Noise considered	Additive white Gaussian noise (AWGN)

**Fig. 11** Manchester coding (cameraman)

the use of BPSK modulation is accompanied through Manchester coding, which also reaffirms the signals after transmission along the extension of AWGN through the Rayleigh Jagir channel. Doing as a joined module, the extra calculation time taken for optional cycles gets dismissed subsequently speeding up the transmission. The image gets more viable along the channel data transfer capacity and sends safely along low calculation time through the packed security network when the module has utilized for the single direction image transmission in MIMO.

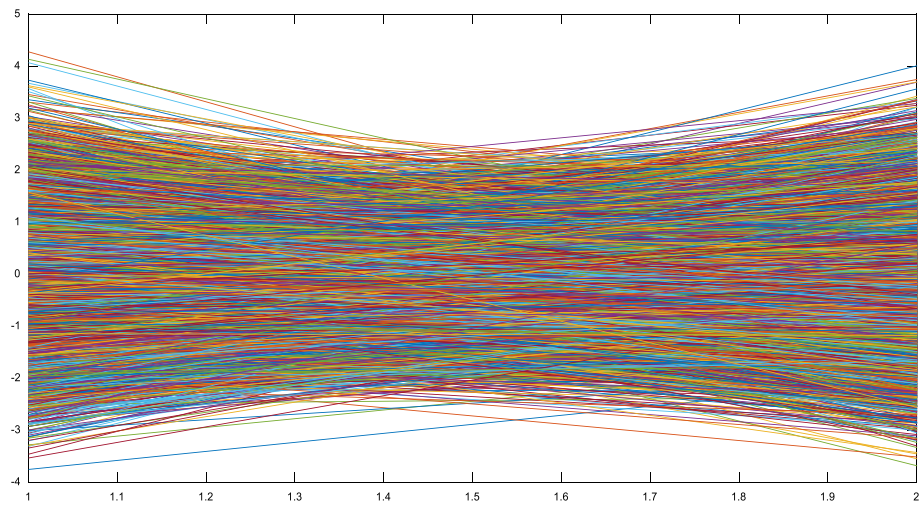


Fig. 12 Addition of AWGN

4 Experimental Results

The proposed two-way transmission of the Corvus Corone module has implemented using the well-known image processing tool MATLAB. We have implemented the proposed model using MATLAB 2015 on Windows 10. The processor is Intel I5 along RAM 8 GB. Through this specification, the detailed explanation of the implementation result and its performance has analyzed in the following section.

4.1 Visual Outcomes

The performance has analyzed in the three stages such as construction, transmission, and reconstruction through the proposed CorvusCorone module that has shown below (Fig. 7).

4.1.1 Construction of Compressed Security

The construction of the compressed security matrix carried out through the proposed CorvusCorone module is shown below.

4.1.1.1 Step 1: Input Image To validate the process, six input images such as cameraman, barbara, man, couple, leena, and ship images are considered for transmission as shown in Fig. 8.

4.1.1.2 Step 2: Selection of Random Matrix Then as stated above in the Sect. 3, for the selection of the random variables regression principles carried out for the input images.

The Fig. 9 above shows the representation of the random matrix made through the random variable regression principles for the six input images.

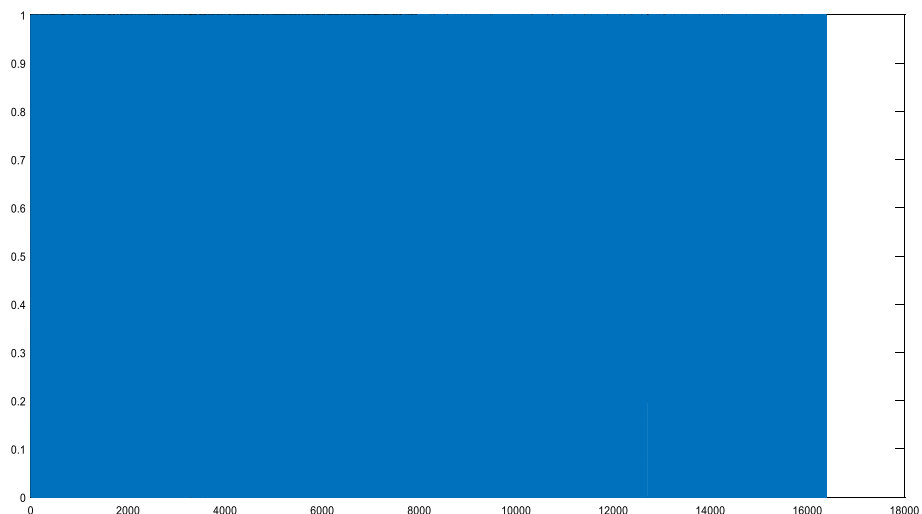


Fig. 13 After Manchester decoding (cameraman)

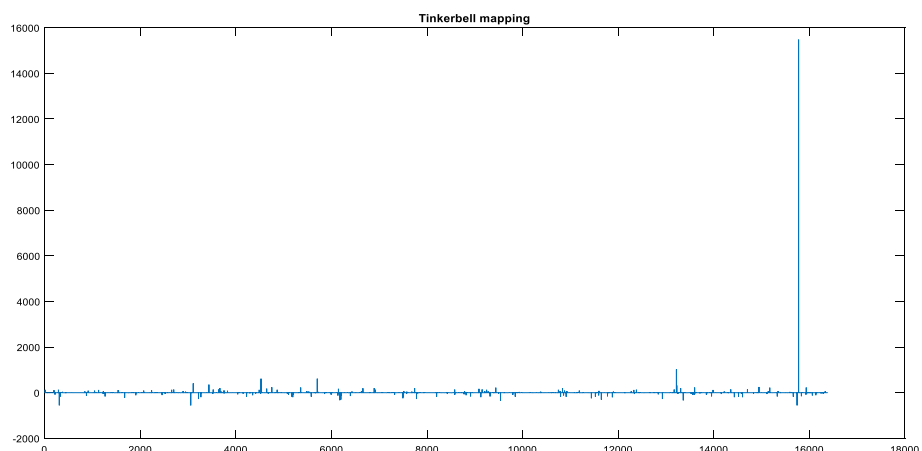


Fig. 14 After regression principle (cameraman)

4.1.1.3 Step 3: Construction of Compressed Security Matrix Through using the regression technique and the tinkering Bell's chaotic values, a security matrix is constructed that can be shown below in Figs. 9 and 10.

4.1.2 Transmission of Compressed Secured Image

The process is executed on considering certain parameters, which are tabulated below in Table 2.

The proposed model executes along 2×2 MU-MIMO channels along 1024 bits in a single packet size. The process was evaluated through the BPSK modulation scheme

Fig. 15 After decrypting the decoded value (cameraman)

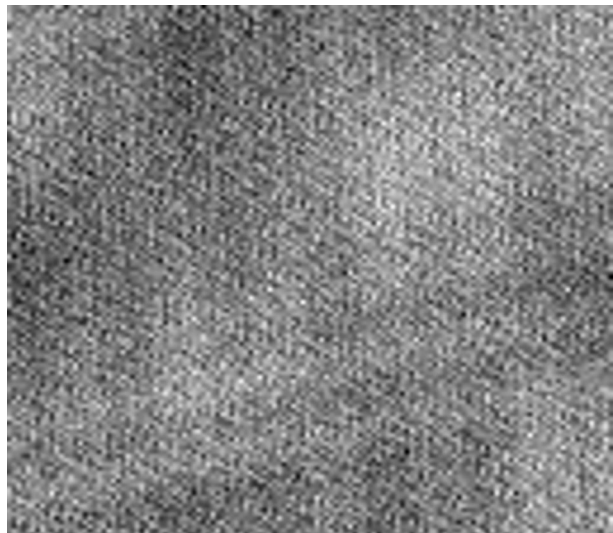


Fig. 16 Received output images

along thousands of people looking at two users at once. The image bits encoded through Manchester Coding are given below (Fig. 11):

When the above signals are transmitted through the channel, the additive white Gaussian noise is added along along the signal. After the addition of those noises, the signals are replaced which is indicated in the following Fig. 12.

Figure 12 shows that Rayleigh changes the signals in the channel other than the AWGN in the channel. Hence to ensure that the reconstruction process is completed which can be explained through the following steps.

4.1.3 Reconstruction of Compressed Security

After AWGN was included in the channel, BER was estimated to retrieve the original signal encoded through Manchester coding. For that Manchester's clock recovery is used to decode the original signal. Then the random variable that is selected at the initial stage is recovered using the forecasting and integrality function of the regression theory (Figs. 13, 14).

After decrypting the random variables through the chaotic values of the tinkering bell would result in the below Fig. 15.

The outcome of the original image after reshaping the obtained value is shown through the Fig. 16.

From Fig. 16, it is proved that using the proposed Corvus Coron module, the input image that is transmitted through the user through a two-way communication channel receives less energy, is safer and encapsulates less energy and Finally reconstructs the output image. The input image is then evaluated seven parameters to evaluate the performance results of the proposed module as shown below.

4.2 Performance Analysis

This section presents the performance evaluation proposed approach in various parameters like PSNR (Peak to Signal Noise Ratio), SNR (Signal to Noise Ratio), Channel Capacity, BER (Bit Error Rate), Time, etc.

Mean Square Error (MSE): The MSE is the cumulative squared error between the compressed and the original image

$$MSE = \frac{1}{MN} \sum_{y=1}^M \sum_{x=1}^N [I(x, y) - I'(x, y)]^2 \quad (19)$$

where $I(x, y)$ is the original image, $I'(x, y)$ is the approximate version (which is the actually decompressed image) and M is the dimensions of N images. The difference between $I(x, y)$ and $I'(x, y)$ will give error. Here, dimensions of M, N image.

Root Mean Squared Error (RMSE): Root mean square was calculated through taking the root of mean square error:

$$RMSE = \sqrt{\text{Mean squared error}} \quad (20)$$

Mean Absolute Error (MAE): Mean Absolute Error takes the mean difference of the absolute values of the error

$$MAE = \frac{1}{\text{Total number of bits}} \sum_{1}^{\text{Total number of bits}} |I(x, y) - I'(x, y)| \quad (21)$$

Bit Error Rate (BER): It is defined as during transmission, the number of bit errors is the number of received bits of a data stream on the communication channels that have been changed due to noise, interference, distortion:

$$BER = \frac{\text{Number of error}}{\text{Number of bits sent}} \quad (22)$$

Symbol Error Rate (SER): It can be said as the amount of errors present in each symbol, decoded at the receiver end. The relation between symbol error rate and bit error rate is as below

$$SER = (\log_2 M) * BER \quad (23)$$

where M is the number of signals, $M=2^k$, k is the number of bits transmitted.

Peak to Signal Noise Ratio: It is defined as a peak signal to noise ratio between the input and output signals.

$$PSNR = 20 * \log_{10} (255 / \sqrt{MSE}) \quad (24)$$

Table 3 Performance evaluation for the proposed module in terms of PSNR, SNR and channel capacity

Images	PSNR	Normalized SNR	Channel capacity	Images	PSNR	Normalized SNR	Channel capacity
Couple	41.7653	1.0532	96.7194	Lena	41.9455	1.0486	96.7172
Barbara	41.7718	1.0376	96.7194	Man	41.1403	0.9922	96.7183
Cameraman	33.7585	1.0562	96.5173	Ship	42.3830	1.0365	96.7133

Table 4 Performance evaluation of the proposed module based on channel state information

S. nos.	Images	No CSI		Along CSI	
		Ergodic capacity	Outage capacity	Ergodic capacity	Outage capacity
1	Couple	32.9593	30.3737	24.9593	22.3798
2	Barbara	33.8944	31.2659	25.6541	23.8478
3	Cameraman	35.3654	32.8946	22.6365	20.5484
4	Lena	35.6554	32.4914	23.64415	20.9854
5	Man	33.9854	31.8944	25.2846	21.3565
6	Ship	36.3454	30.8458	24.3655	22.6794

Peak Signal to Noise Ratio is the ratio of maximal intensity of the image to the amount of error present as in terms of mean square.

Correlation Coefficient: Correlation provides an association between the two variables as well as its relationship, a +ve correlation value indicates better relation while a -ve correlation value least correlation. The value of correlation varies from +1 to -1; we considered three correlation types.

Spearman Correlation: Spearman rank correlation is a one of the correlation methods that is used to measure the degree of association between the two variables.

$$\rho = 1 - \frac{6 \sum d_i^2}{n(n^2 - 1)} \quad (25)$$

where ρ -Spearman's rank correlation, d_i , is the difference between the ranks of the variances and n is the number of data seen in the image Pearson correlation: Pearson action correlation is a correlation statistic to measure the degree of relationship between linear relational variables.

$$\gamma = \frac{N \sum xy - \sum (x)(y)}{\sqrt{[N \sum x^2 - \sum (x^2)][N \sum y^2 - \sum (y^2)]}} \quad (26)$$

where γ is the Pearson correlation coefficient, N would be the total number of observed data from the image.

$\sum xy$ is the sum of the product of paired scores,
 $\sum x$ is the sum of x scores,

Table 5 Performance evaluation of the proposed module based time and BER

Image	Time	BER	Image	Time	BER
Couple	1.4056949	0.0003052	Lena	1.4527804	0.0003032
Barbara	1.4202456	0.0003089	Man	1.5079328	0.0003084
Camera-man	1.5236545	0.0003022	Ship	1.5636474	0.0003062

Table 6 Performance of MSE, RMSE, and MAE

Images	MSE	RMSE	MAE
Barbara	340.234	18.4454	14.7186
Cameraman	555.099	23.5605	18.8618
Couple	208.205	14.4296	11.5139
Ship	228.242	15.1077	11.9529
Lena	268.644	16.3904	12.9067
Man	287.221	16.9476	13.417

$\sum y$ is the sum of y scores,

$\sum x^2$ is the sum of squared x scores.

$\sum y^2$ is the sum of squared y scores.

Kendall Correlation: Kendall rank correlation is a test that measures the strength of dependence between two variables.

$$\tau = \frac{n_c - n_d}{\frac{1}{2}n(n-1)} \quad (27)$$

where n_c is the number of elements which are ordered in similar manner, n_d is the number of elements which are ordered in dissimilar manner.

Moment Generating Function (MGF): Moments describes about the image content along respect to its axes, they help capture the global and detailed geometric information about the image. Considering a moment of order (p, q) spread over a plane S, along basis function $\Psi_{p,q}$ which in turn produces a weighted description over the plane same ‘s’. These functions have properties that get passed to the moments, producing descriptions which are invariant under translation, orientation and rotation.

$$M_{pq} = \sum_x \sum_y \Psi_{pq}(x, y) P_{xy}; \quad p, q = 0, 1, 2, \dots, \infty \quad (28)$$

where P_{xy} is the multiple of image intensity over each pixel.

Structural Similarity (SSIM): Structural similarity is a similarity measurement index that is useful for finding the similarity among the predicted/reconstructed/compressed image along a reference /uncompressed/original image as reference.

$$SSim(x, y) = \frac{(2\mu_x\mu_y + c_1)(2\sigma_{xy} + c_2)}{(\mu_x^2 + \mu_y^2 + c_1)(\sigma_x^2 + \sigma_y^2 + c_2)} \quad (29)$$

Fig. 17 Performance proposed models performance in terms of Channel capacity, Normalized SNR and PSNR respectively

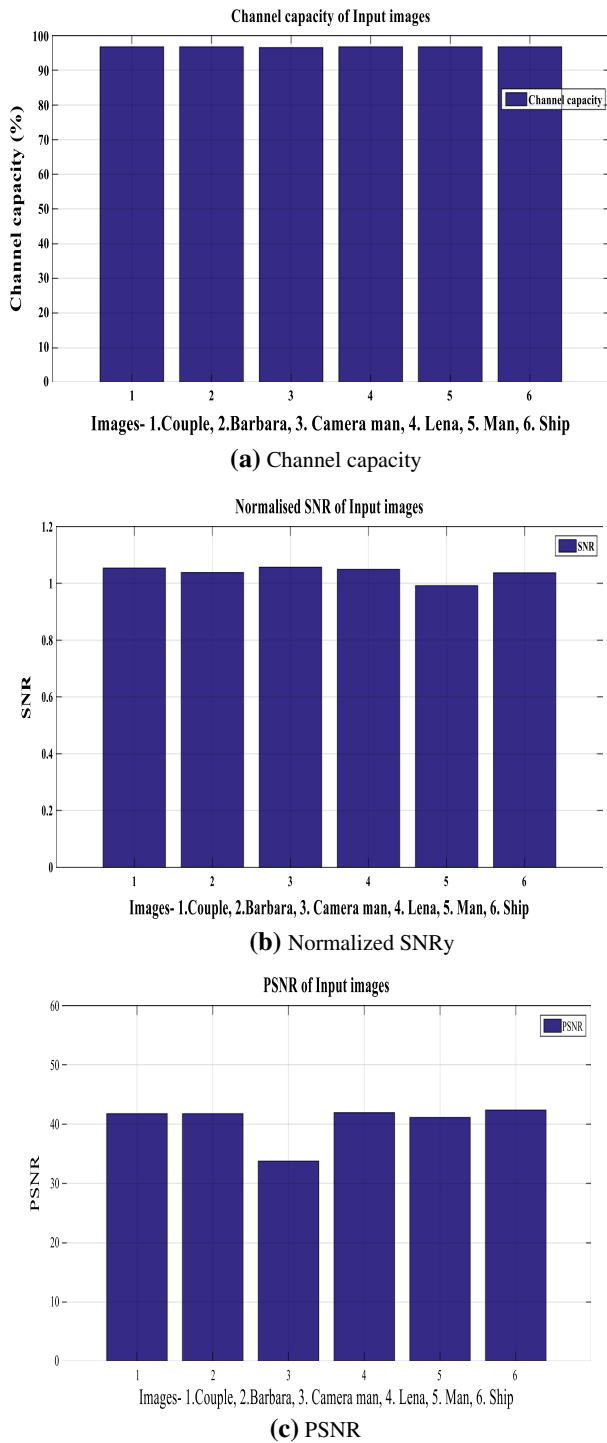
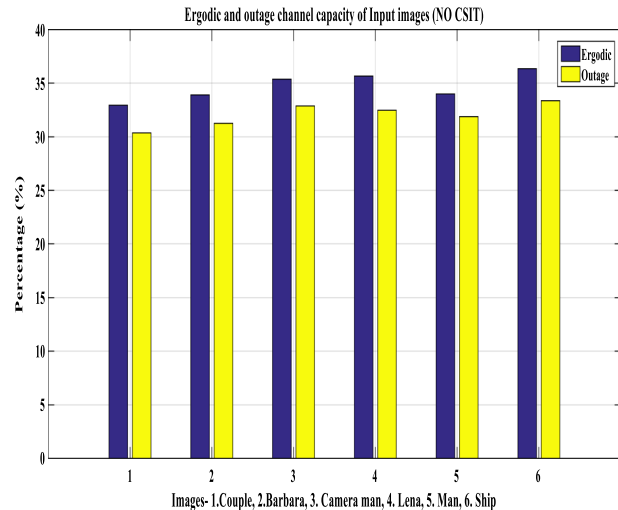
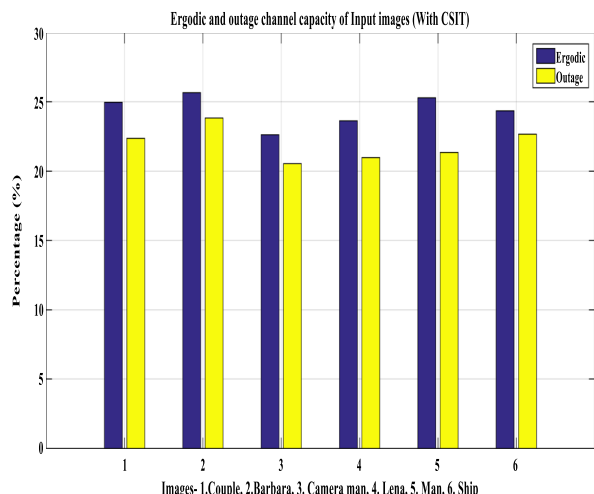


Fig. 18 Corresponds to the proposed models performance in terms of channel capacity (Ergodic and Outage) along no channel side information and along channel side information



(a) Ergodic & Outage performance along no CSI



(b) Ergodic & Outage performance along CSI

where \bar{x}_x , μ_{xy} , σ_{2x} , y_2y are the averages and versions of x and y respectively. σ_{xy} is covariant of x and y , $c1=(k1L)^2$, $c2=(k2L)^2$ are variables for stabilization, L will be the dynamic range of pixel values (2 bits per pixel-1 $k1=0.01$ and $k2=0.03$;

Signal to Noise Ratio (SNR): SNR is defined as the ratio of the average signal value to the standard deviation of the background values. The noise ratio (SNR) can be used as a measure of signal sensitivity; The value returns to normal when the SNR is divided through its dimensions

$$\text{SNR} = \mu_{xy}/\sigma_{xy} \quad (30)$$

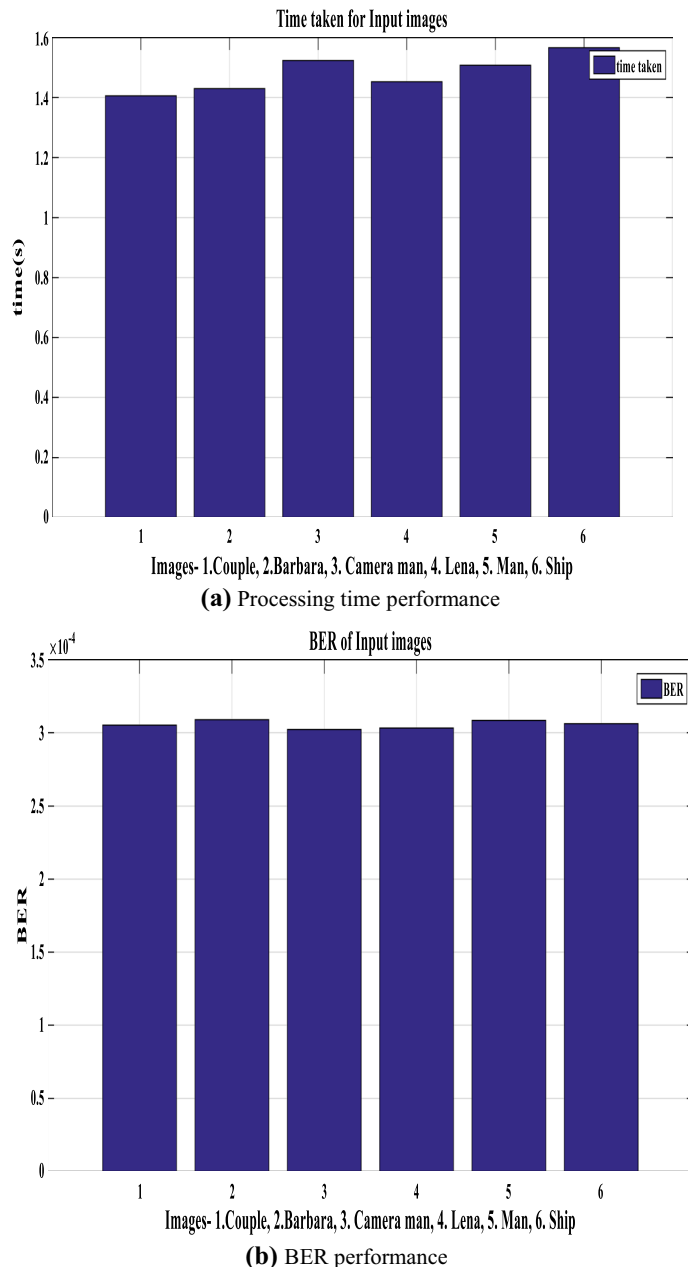


Fig. 19 The proposed models performance in terms of bit error rate and time taken

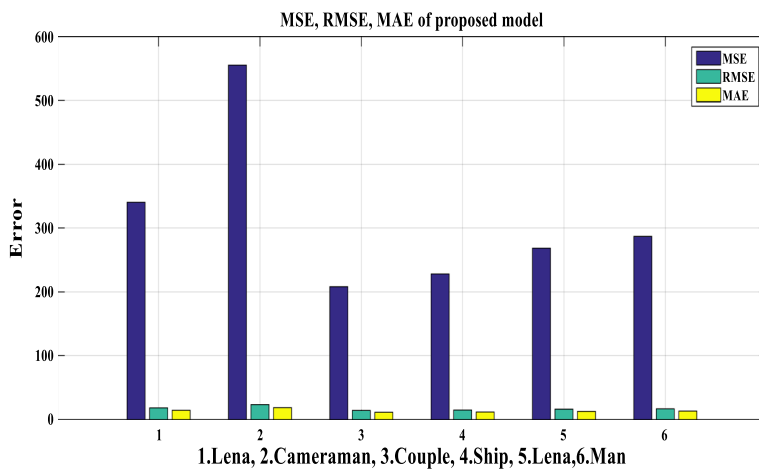


Fig. 20 Proposed model's mean squared error, root mean squared error and mean absolute error

Table 7 Performance of SER

Images	SER
Barbara	8.46127×10^{-5}
Cameraman	8.462147×10^{-5}
Couple	8.46185×10^{-5}
Ship	8.46156×10^{-5}
Lena	8.46173×10^{-5}
Man	8.46121×10^{-5}

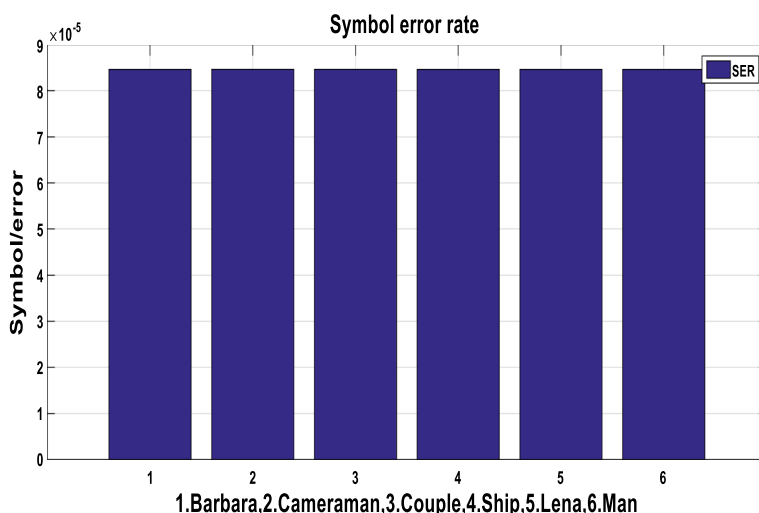


Fig. 21 Symbol error rate the input images

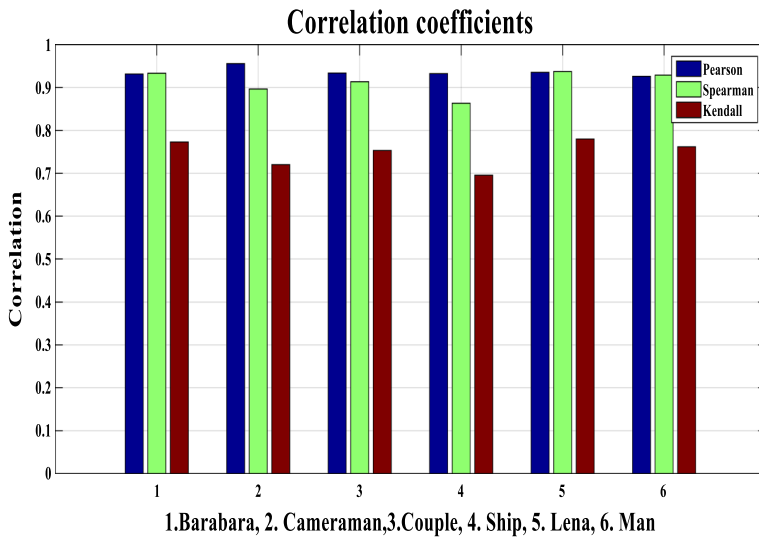


Fig. 22 Correlation coefficients the input images

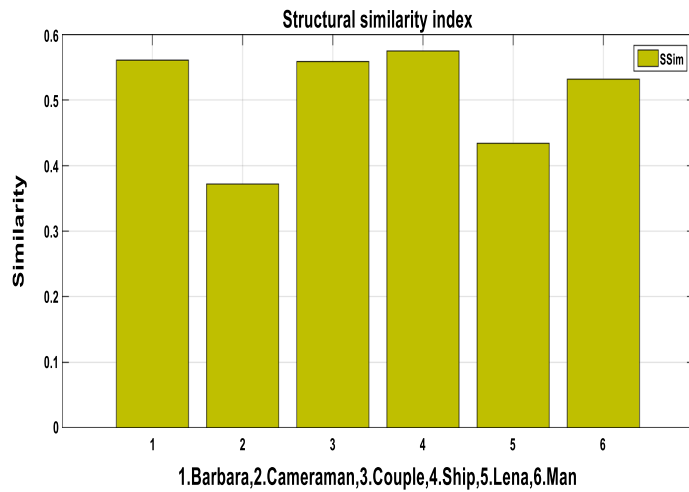


Fig. 23 Structural similarity of the input images

Table 8 Performance of SER

Images	Pearson	Spearman	Kendall
Barbara	0.931310	0.933131	0.773216
Cameraman	0.955553	0.896281	0.720296
Couple	0.933510	0.913297	0.753469
Ship	0.932259	0.863025	0.695773
Lena	0.935225	0.937098	0.780140
Man	0.925844	0.928689	0.762114

Table 9 Structural similarity index

Images	SSIM
Barbara	0.560887
Cameraman	0.371988
Couple	0.558823
Ship	0.57498
Lena	0.434309
Man	0.531887

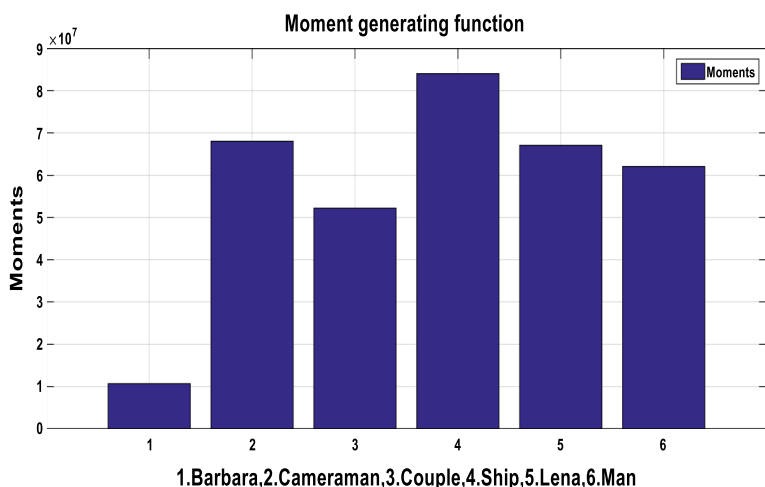
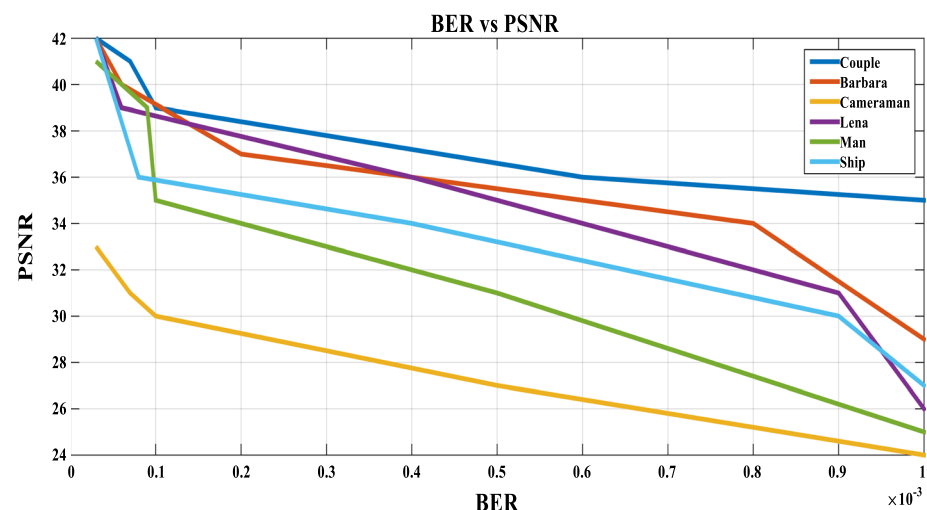
**Fig. 24** MGF of the input images**Fig. 25** BER versus PSNR of the input images

Table 10 Moment generating function value

Images	MGF
Barbara	$1.06838 \times e^{07}$
Cameraman	$6.80244 \times e^{07}$
Couple	$5.22359 \times e^{07}$
Ship	$8.40572 \times e^{07}$
Lena	$6.7065 \times e^{07}$
Man	$6.21233 \times e^{07}$

Table 11 BER versus PSNR

	Couple	Barbara	Cameraman	Lena	Man	Ship
PSNR	42	42	33	42	41	42
	41	40	31	39	39	36
	39	37	30	36	35	34
	36	34	27	31	31	30
	35	29	24	26	25	27
BER	$0.0305 \times e^{-5}$	$0.0308 \times e^{-5}$	$0.0302 \times e^{-5}$	$0.0303 \times e^{-5}$	$0.0308 \times e^{-5}$	$.0306 \times e^{-5}$
	$0.0714 \times e^{-5}$	$0.0645 \times e^{-5}$	$0.0727 \times e^{-5}$	$0.0667 \times e^{-5}$	$0.0911 \times e^{-5}$	$0.0842 \times e^{-5}$
	$0.0112 \times e^{-4}$	$0.0247 \times e^{-4}$	$0.0185 \times e^{-4}$	$0.0478 \times e^{-4}$	$0.0136 \times e^{-4}$	$0.0458 \times e^{-4}$
	$0.0664 \times e^{-4}$	$0.0845 \times e^{-4}$	$0.0532 \times e^{-4}$	$0.0956 \times e^{-4}$	$0.0567 \times e^{-4}$	$0.0964 \times e^{-4}$
	$0.104 \times e^{-3}$	$0.107 \times e^{-3}$	$0.103 \times e^{-3}$	$0.108 \times e^{-3}$	$0.108 \times e^{-3}$	$0.107 \times e^{-3}$

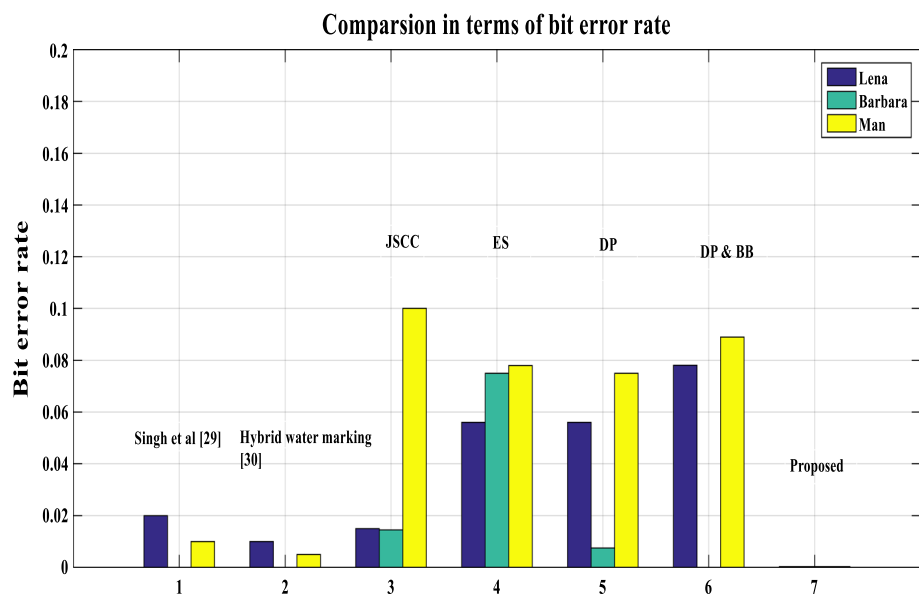
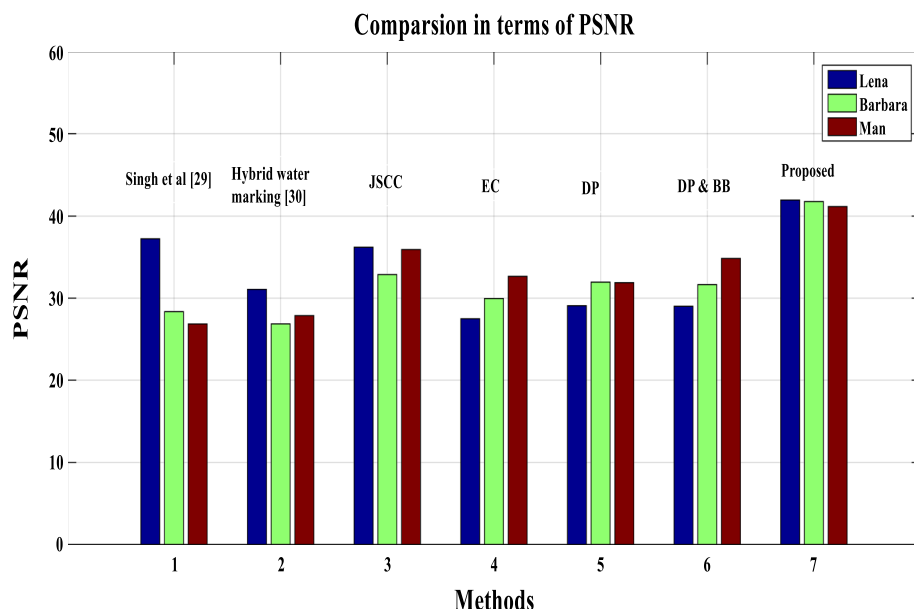
**Fig. 26** Comparison of BER along the existing techniques

Table 12 Comparison of BER along the existing techniques

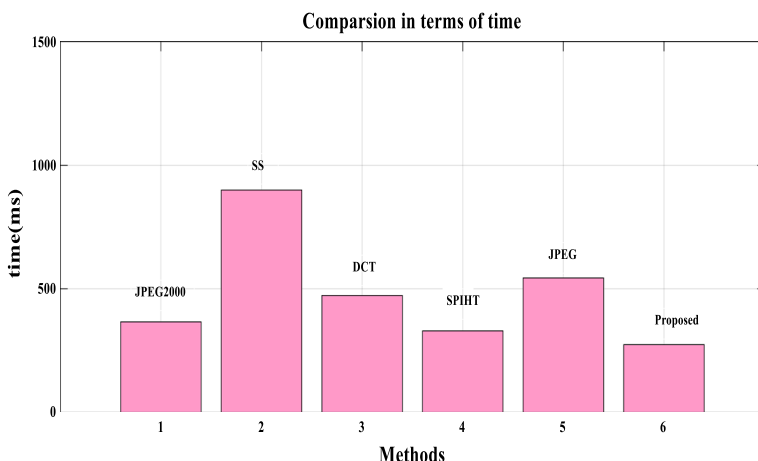
Methods	Lena	Barbara	Man
Singh et al. [28]	0.02	0	0.01
Hybrid water marking [29]	0.01	0	0.005
JSCC	0.015	0.0145	0.1
ES	0.0056	0.075	0.078
DP	0.056	0.0075	0.0075
DP and BB	0.0781	0	0.089
Proposed	0.0003032	0.0003089	0.0003054

**Fig. 27** Comparison of PSNR along the existing techniques**Table 13** Comparison of PSNR along the existing techniques

Methods	Lena	Barbara	Man
<i>Peak to signal noise ratio</i>			
Singh et al. [28]	37.23	28.35	26.85
Hybrid water marking [29]	31.06	26.86	27.86
JSCC	36.20	32.87	35.92
ES	27.48	29.95	32.65
DP	29.08	31.95	31.88
DP and BB	29.01	31.65	34.83
Proposed	41.9455	41.7718	41.154

Table 14 Comparison of communication time along the existing techniques

Methods	Time consumption (ms)
JPEG2000	366
SS	900
DCT	473
SPIHT	331
JPEG	544
Proposed	275

**Fig. 28** Comparison of communication time along the existing techniques**Table 15** Comparison of energy consumption along the existing techniques

Methods	Energy consumption (mJ)	% Energy saving
Lucire et al. [31]	1252.6	87.47
Nasri et al. [32]	1252.6	87.47
WMSN	411.3	95.88
Proposed	386.9	98.54

Table 3 demonstrates the outcome of PSRN, SNR and Channel capacity parameters for different images tested.

From Tables 3, 4, and 5, analyzing the parameters such as PSNR, BER, normalized SNR, channel capacity, argotic and outage values considering along and without CSI (Channel State Information), time, the proposed CorvusCorone module, shows the effective values for the six images (Table 6).

The above Fig. 17 shows the mean squared error, root mean squared error and mean absolute error of the proposed methodology. The values squared errors points the value

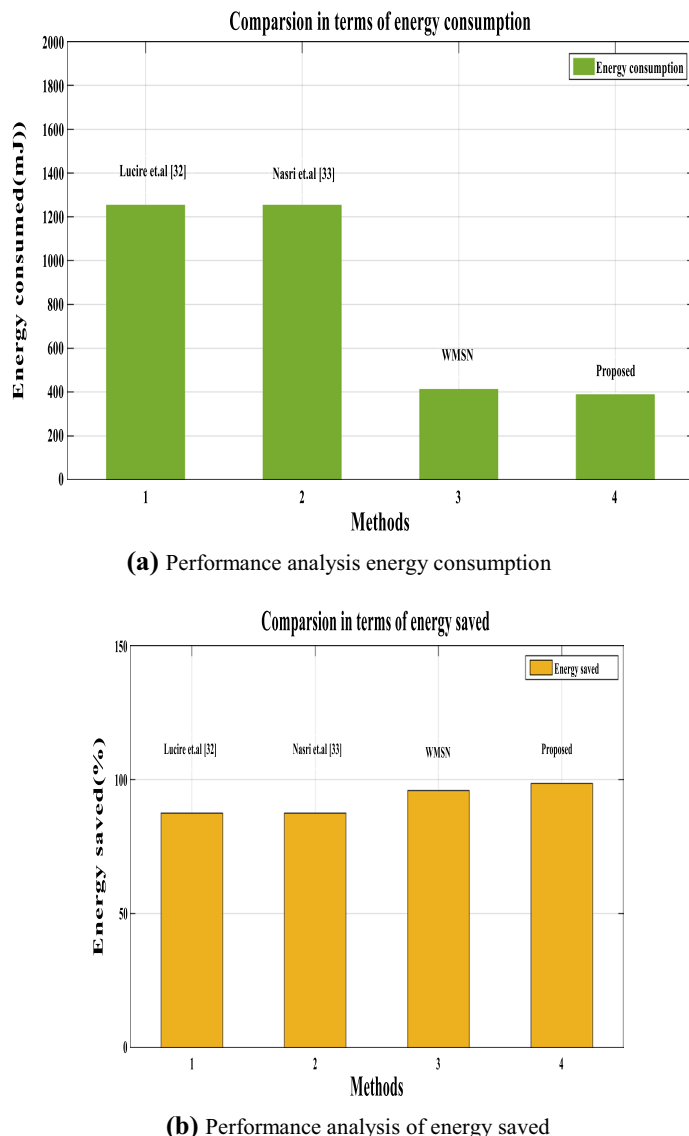


Fig. 29 Comparison of energy consumption and energy saved along the existing techniques respectively

of 314.6705 and 17.4802 along the average errors 13.895 of shows better efficient channel capacity (Figs. 18, 19, 20; Table 7).

The above table describes the symbol error rate obtained for those input images fed to the proposed system. It can be seen that the symbol error rate close to 8.4×10^5 for all the images, suggesting that all the 6 images have close resemblance in SER (Figs. 21, 22, 23).

The above correlation coefficients are all positive indicating the better correlation among the reconstructed and original input image. Considering all the correlation, the maximal correlation happened for the Lena image, where as the lesser correlation occurred for the ship (Tables 8, 9).

The table describes the SSIM obtained for the 6 input images, along the maximum SSIM seen for the doubles image and the least for the cameraman (Figs. 24, 25).

The Table 10 describes the MGF obtained for the 6 input images, the image Ship had the highest MGF of 8.40572×10^7 .

The above Table 11 describes the BER versus PSNR of all the 6 input images and their corresponding line graphs, it can be seen that the PSNR values remains high when BER is low, and the PSNR value decreases when BER turns to be high.

4.2.1 Similar Method Analysis

This section presents the comparative study of proposed model along recent similar methods.

From Fig. 26 and Table 12, the proposed methodology combined Singh et al. Hybrid watermarking, JSCC, ES, DP, and DP along their BER in the context of BB, compared to other existing methodologies. It seems that Singh et al.'s existing methodology and hybrid watermarking techniques along 0.02, 0 and 0.01 make a big difference for their images Leena and Barbara. 0. It has a value of 0.303032 as compared to the proposed method. Lina and 0.0003089 for Barbara show that due to proper modulation and transmission the module becomes effective.

From Fig. 27 and Table 13, the proposed methodology compared the other two existing methodologies along reference to other PSNRs. Our model has a PSNR value of 41.9455 for Lina 41.7718 for Barbara compared to some of the proposed methodology and 41.154 works well compared to others to show the proposed system.

Communication time is the total time it takes for a communication process to occur when transmitting user data from one location to another. Table 14 and Fig. 27 show the results of communication analysis along existing methods.

From Figs. 28 and Table 14, the proposed methodology compares to other existing methodologies in terms of their communication time. It seems that the current working of JPEG2000, SS, DCT, SPIHT, JPEG is 366, 900, 473, 331, 544 ms. This is compared to the proposed methodology along a value of 275 ms and shows that due to proper modulation and transmission the module becomes effective and possesses shorter communication time.

Further we computed the energy consumption for comparative analysis. It is the total amount of energy consumed during the transmission process. Table 15 and Fig. 29 demonstrate its outcome.

From Fig. 29a, b, the proposed methodology compared to other existing methodology in terms of their energy consumption and energy saving. The current methodology seems to have higher energy consumption and lower N-allergen savings. It consumes

386 MJ of energy as compared to the proposed methodology and saves energy of 98.54% indicating efficient energy usage through the proposed module.

5 Conclusion and Future Work

The energy-efficient transmission along a security problem in the two-way image transmission was challengingly solved through the proposed Corvus Corone module through their compressed security matrix which increases the security, consumes less energy, and prevents the signals from unwanted noise. The evaluation and comparison results paraded that the proposed module achieves the process within 1.42 s along an enhanced channel capacity of 96.684 and leads to the less BER value of 0.0003 compared to the other techniques respectively.

Funding No funding.

Declarations

Conflict of interest All authors declares that they has no conflict of interest.

Ethical approval This article does not contain any studies along human participants performed through any of the authors.

References

- Chandra, M., Agarwal, D., & Bansal, A. (2016). Image transmission through wireless channel: A review. In *2016 IEEE 1st international conference on power electronics, intelligent control and energy systems (ICPEICES)*. <https://doi.org/10.1109/icpeices.2016.7853121>.
- Mahajan, H. B., & Badarla, A. (2018). Application of internet of things for smart precision farming: Solutions and challenges. *International Journal of Advanced Science and Technology*, 2018, 37–45.
- Talukder, K., & Harada, K. (2010). Haar wavelet based approach for image compression and quality assessment of compressed image. *IAENG International Journal of Applied Mathematics*, 36.
- Hepper, D. (2014). *Film grain noise superimposition for film grain management* (pp. 252–255). <https://doi.org/10.1109/ICCE.2014.6775992>.
- Yang, J., He, S., Lin, Y., & Lv, Z. (2015). Multimedia cloud transmission and storage system based on internet of things. *Multimedia Tools and Applications*, 76(17), 17735–17750. <https://doi.org/10.1007/s11042-015-2967-9>.
- Qaisar, S., Bilal, R. M., Iqbal, W., Naureen, M., & Lee, S. (2013). Compressive sensing: From theory to applications, a survey. *Journal of Communications and Networks*, 15, 443–456. <https://doi.org/10.1109/JCN.2013.000083>.
- Zhang, Y., Zhang, L. Y., Zhou, J., Liu, L., Chen, F., & He, X. (2016). A review of compressive sensing in information security field. *IEEE Access*, 4, 2507–2519. <https://doi.org/10.1109/access.2016.2569421>.
- Marvasti, F., Amini, A., Haddadi, F., Soltanolkoltabi, M., Khalaj, B. H., Aldroubi, A., & Chambers, J. (2012). A unified approach to sparse signal processing. *EURASIP Journal on Advances in Signal Processing*. <https://doi.org/10.1186/1687-6180-2012-44>.
- Karakus, C., Gurbuz, A. C., & Tavli, B. (2013). Analysis of energy efficiency of compressive sensing in wireless sensor networks. *IEEE Sensors Journal*, 13(5), 1999–2008. <https://doi.org/10.1109/jsen.2013.2244036>.
- Zhang, J., Zhao, D., Zhao, C., Xiong, R., Ma, S., & Gao, W. (2012). Image compressive sensing recovery via collaborative sparsity. *IEEE Journal on Emerging and Selected Topics in Circuits and Systems*, 2(3), 380–391. <https://doi.org/10.1109/jetcas.2012.2220391>.

11. Fornasier, M. (Ed.). (2010). Compressive sensing and structured random matrices. *Radon Series on Computational and Applied Mathematics*. <https://doi.org/10.1515/9783110226157.1>.
12. Tropp, J. A., & Gilbert, A. C. (2007). Signal recovery from random measurements via orthogonal matching pursuit. *IEEE Transactions on Information Theory*, 53(12), 4655–4666. <https://doi.org/10.1109/tit.2007.909108>.
13. Candès, E. J., & Tao, T. (2006). Near-optimal signal recovery from random projections: Universal encoding strategies? *IEEE Transactions on Information Theory*, 52(12), 5406–5425. <https://doi.org/10.1109/tit.2006.885507>.
14. Otazo, R., Candès, E., & Sodickson, D. K. (2014). Low-rank plus sparse matrix decomposition for accelerated dynamic MRI along separation of background and dynamic components. *Magnetic Resonance in Medicine*, 73(3), 1125–1136. <https://doi.org/10.1002/mrm.25240>.
15. Haupt, J., Bajwa, W. U., Raz, G., & Nowak, R. (2010). Toeplitz compressed sensing matrices along applications to sparse channel estimation. *IEEE Transactions on Information Theory*, 56(11), 5862–5875. <https://doi.org/10.1109/tit.2010.2070191>.
16. Ponuma, R., & Amutha, R. (2017). Compressive sensing based image compression–encryption using Novel 1D-Chaotic map. *Multimedia Tools and Applications*, 77(15), 19209–19234. <https://doi.org/10.1007/s11042-017-5378-2>.
17. Paredes, J. L., Arce, G. R., & Wang, Z. (2007). Ultra-wideband compressed sensing: Channel estimation. *IEEE Journal of Selected Topics in Signal Processing*, 1(3), 383–395. <https://doi.org/10.1109/jstsp.2007.906657>.
18. Trzasko, J., & Manduca, A. (2009). Highly undersampled magnetic resonance image reconstruction via homotopic ℓ_0 -minimization. *IEEE transactions on Medical Imaging*, 28, 106–121. <https://doi.org/10.1109/TMI.2008.927346>.
19. Watteyne, T., Lanzisera, S., Mehta, A., & Pister, K. (2010). *Mitigating multipath fading through channel hopping in wireless sensor networks*. (pp. 1–5). <https://doi.org/10.1109/ICC.2010.5502548>.
20. Kohno, R., Meidan, R., & Milstein, L. B. (1995). Spread spectrum access methods for wireless communications. *IEEE Communications Magazine*, 33(1), 58–67. <https://doi.org/10.1109/35.339882>.
21. El-Bakary, E. M., Hassan, E. S., Zahran, O., El-Dolil, S. A., & El-Samie, F. E. A. (2012). Efficient image transmission along multi-carrier CDMA. *Wireless Personal Communications*, 69(2), 979–994. <https://doi.org/10.1007/s11277-012-0622-6>.
22. Almagdab, A. A., Abdurrahman, A. B., Nasir, I. A., & Abughres, W. S. (2020). Image transmission over erroneous wireless mobile channels using HQAM techniques. *Journal of Pure & Applied Sciences*, 19(3), 7–12. <https://doi.org/10.51984/jopas.v19i3.773>.
23. Liao, X., Li, K., & Yin, J. (2016). Separable data hiding in encrypted image based on compressive sensing and discrete Fourier transform. *Multimedia Tools and Applications*, 76(20), 20739–20753. <https://doi.org/10.1007/s11042-016-3971-4>.
24. Ahmad, J., Khan, M. A., Hwang, S. O., & Khan, J. S. (2016). A compression sensing and noise-tolerant image encryption scheme based on chaotic maps and orthogonal matrices. *Neural Computing and Applications*, 28(S1), 953–967. <https://doi.org/10.1007/s00521-016-2405-6>.
25. Capacity of Burst Noise-Erasure Channels Along and Without Feedback and Input Cost. (2018). *IEEE Transactions on Information Theory* (p. 1). <https://doi.org/10.1109/tit.2018.2862354>.
26. Tarique, M. (2016). Performances of orthogonal wavelet division multiplex (OWDM) system under AWGN, Rayleigh & Ricean channel conditions. *International Journal of Computer Networks and Communications*. <https://doi.org/10.5121/ijcnc.2016.8307>.
27. Li, L., Xu, D., Peng, H., Kurths, J., & Yang, Y. (2017). Reconstruction of complex network based on the noise via QR decomposition and compressed sensing. *Scientific Reports*. <https://doi.org/10.1038/s41598-017-15181-3>.
28. Singh, A. K. (2016). Improved hybrid algorithm for robust and imperceptible multiple watermarking using digital images. *Multimedia Tools and Applications*, 76(6), 8881–8900. <https://doi.org/10.1007/s11042-016-3514-z>.
29. Singh, A. K., Dave, M., & Mohan, A. (2015). Hybrid technique for robust and imperceptible multiple watermarking using medical images. *Multimedia Tools and Applications*, 75(14), 8381–8401. <https://doi.org/10.1007/s11042-015-2754-7>.
30. Mahajan, H. B., Badarla, A., & Junnarkar, A. A. (2020). CL-IoT: Cross-layer Internet of Things protocol for intelligent manufacturing of smart farming. *Journal of Ambient Intelligence and Humanized Computing*. <https://doi.org/10.1007/s12652-020-02502-0>.
31. Lecuire, V., Duran-Faundez, C., & Krommenacker, N. (2008). Energy efficient image transmission in sensor networks. *International Journal of Sensor Networks*, 4, 37–47.

32. Nasri, M., Helali, A., Sghaier, H., & Maaref, H. (2010). Adaptive image transfer for wireless sensor networks (WSN). In *IEEE 5th International conference on design and technology of integrated systems in nanoscale era (DTIS)* (pp. 1–7).

Publisher's Note Springer Nature remains neutral with regard to jurisdictional claims in published maps and institutional affiliations.



Dr. Bilal Alhayani He graduated his Ph.D. in Engineer Electronics and Communication Department in 2019 from Yildiz Technical University, Istanbul, Turkey. He received the B.Sc. degree in Laser Engineering from university of Technology –Baghdad, Iraq, and the M.Sc. degree in electronics and telecommunication engineering and electromagnetic from University of Pune, India from 2011 to 2013. His general research interests lie in signal processing and communication theory and signal coding on wireless communication and image processing specific research area include cooperative and MIMO communication techniques, security, PHY and MAC, 5G wireless systems, wireless IoT technologies, network virtualization, network slicing, graph signal processing, pattern recognition (face recognition, Iris recognition, finger print).



Sara Taher Abbas she is a Lecturer at Imam Ja'afar Al-Sadiq University. She received B.Sc. from University of Technology, Department of Computer Engineering and Information Technology in 2009. She graduated her M.Sc. in 2020 from University of Technology, Department of Computer Engineering. Her general research interests lie in wireless sensors network (WSN), IOT, Network Security, Wireless Network, Artificial intelligent (Fuzzy Logic, Neural Network).



Dr. Husam Jasim Mohammed he is a Senior Lecturer at Imam Ja'afar Al-Sadiq University, Department of Business Administration. He graduated his Ph.D. in 2018 from the Department of Decision Sciences, School of Quantitative Sciences, Universiti Utara Malaysia (UUM). His research interest is Operational Research in terms of using more advanced optimization techniques. My area of research is focused on decision science especially in quantitative science for decision making and multi-criteria decision making (MCDM).



Dr. Hemant B. Mahajan he received B.Sc. (Comp. Sci.) degree from Savitribai Phule Pune University, India, in 2003, M. Sc. (Comp. Sci.) from Savitribai Phule Pune University, India, in 2006. He is currently pursuing doctorate in Computer Science from the University of Technology (UOT), India. He is working as a research analyst and data scientist in Godwit Technologies, Pune (India) since 2008. He is having 12+ years of experience in Research and Development across different domains. His area of expertise includes but is not limited to wireless communications, network security, image processing, biomedical, data mining, cloud computing, signal (audio/video) processing, and machine learning. His current area of interest is IoT-enabled communications, Healthcare 4.0, Industry 4.0, Deep Learning, Artificial Intelligence, and Security. He published 7 articles in peer reviewed journals and 5 Indian patents.

Authors and Affiliations

Bilal Alhayani¹ · Sara Taher Abbas² · Husam Jasim Mohammed³ · Hemant B. Mahajan⁴

Sara Taher Abbas
sara.taher@sadiq.edu.iq

Husam Jasim Mohammed
dr.hussam@sadiq.edu.iq

Hemant B. Mahajan
mahhemant@gmail.com

¹ Yildiz Technical University, Istanbul, Turkey

² Department of Computer Engineering Techniques, College of Information Technology, Imam Ja'afar Al-Sadiq University, Baghdad, Iraq

³ Department of Business Administration, College of Administration Sciences and Financial, Imam Ja'afar Al-Sadiq University, Baghdad, Iraq

⁴ Research Analyst and Data Scientists, University of Technology, Pune, India